PHYSICAL REVIEW D **87,** 073011 (2013)

Neutrino mass matrices with two equalities between the elements or cofactors

S. Dev,[1,2,*] Radha Raman Gautam,[1,†] and Lal Singh[1,‡]

[1]*Department of Physics, Himachal Pradesh University, Shimla 171005, India*

[2]*Department of Physics, School of Sciences, HNBG Central University, Srinagar, Uttarakhand 246174, India*

(Received 7 January 2013; published 23 April 2013)

We study the implications of the existence of two equalities between the elements or cofactors of the neutrino mass matrix. There are 65 structures of this type for each case. Phenomenological implications for unknown parameters like the effective Majorana mass of the electron neutrino and *CP*-violating phases are examined for the viable cases. To illustrate how such forms of the neutrino mass matrices may be realized, we also present a simple A_4 model for one of the classes in each case.

DOI: 10.1103/PhysRevD.87.073011 PACS numbers: 14.60.Pq, 11.30.Hv, 14.60.St

I. INTRODUCTION

After the discovery of neutrino oscillations, there has been tremendous progress in determining neutrino masses and mixings. Recently, the last unknown mixing angle (θ_{13}) has been measured rather precisely [1–5] and its relatively large value has also provided an opportunity for the measurement of *CP*-violating phase δ in the lepton mixing matrix. The rather large value of θ_{13} has also forced modifications of models like tribimaximal (TBM) mixing [6] that predict $\theta_{13} = 0$, by considering deviations from TBM mixing. On the other hand, schemes like zero textures [7,8], vanishing minors [9], and hybrid textures [10], which do not predict definite values of mixing angles but do induce relations between neutrino masses and mixing angles, readily accommodate a nonzero and relatively large value of θ_{13}. However, the currently available data on neutrino masses and mixings are insufficient for an unambiguous reconstruction of the neutrino mass matrix. The existing data cannot, without some additional assumptions, determine all the elements of the Yukawa coupling matrices for the neutrinos. Thus, theoretical ideas such as zero textures [7,8], vanishing minors [9], and hybrid textures [10], which restrict the structure of the neutrino mass matrix (M_ν), are important for guiding future searches.

In this work, we systematically study the implications of the existence of two equalities between elements (TEE) of the neutrino mass matrix or two equalities between cofactors (TEC) of the neutrino mass matrix. There are 65 such possibilities in each case which have been listed in Table I. We find that two equalities between the elements of M_ν can be obtained through type-II seesaw mechanism [11], whereas two equalities between cofactors of M_ν arise from type-I seesaw mechanism [12].

*dev5703@yahoo.com
†gautamrrg@gmail.com
‡lalsingh96@yahoo.com

In the framework of type-I seesaw mechanism, the effective Majorana neutrino mass matrix is given by

$$M_\nu = -M_D M_R^{-1} M_D^T, \tag{1}$$

where M_D is the Dirac neutrino mass matrix and M_R is the right-handed Majorana mass matrix. In the diagonal basis for M_D, the zero textures of M_R show as zero minors in M_ν [9]. Here, we consider the possibility that M_R has two equal elements and M_D is proportional to the unit matrix. Such M_D and M_R will give rise to the neutrino mass matrix M_ν, which has two equalities between the cofactors of M_ν and the two equalities of cofactors in M_ν correspond to the equal elements in M_R. Two equalities between cofactors, in other words, can be seen as two equalities between elements of the inverse of M_ν. Thus, effectively we are studying all the possible cases of two equalities between the elements of M_ν and M_ν^{-1}. The condition of two equalities between the elements or cofactors of M_ν implies constraints on the parameters of the neutrino sector which lead to a restricted parameter space for these observables. To demonstrate how such forms of M_ν can be realized, we also present a simple A_4 model for one of the texture structures in each case.

II. FORMALISM

We reconstruct the neutrino mass matrix in the flavor basis, assuming neutrinos to be Majorana particles. In this basis, a complex symmetric neutrino mass matrix can be diagonalized by a unitary matrix V' as

$$M_\nu = V' M_\nu^{\rm diag} V'^T, \tag{2}$$

where $M_\nu^{\rm diag} = {\rm diag}(m_1, m_2, m_3)$.

The unitary matrix V' can be parametrized as

$$V' = P_l V \quad \text{with} \quad V = U P_\nu, \tag{3}$$

where [13]

TABLE I. Sixty-five possible texture structures of M_ν or M_R with two equalities.

	A	B	C	D	E	F
I	$\begin{pmatrix} a & a & a \\ a & d & e \\ a & e & f \end{pmatrix}$	$\begin{pmatrix} a & b & a \\ b & a & e \\ a & e & f \end{pmatrix}$	$\begin{pmatrix} a & b & c \\ b & a & a \\ c & a & f \end{pmatrix}$	$\begin{pmatrix} a & b & c \\ b & d & a \\ c & a & a \end{pmatrix}$	$\begin{pmatrix} a & b & b \\ b & d & e \\ b & e & a \end{pmatrix}$	$\begin{pmatrix} a & b & b \\ b & b & e \\ b & e & f \end{pmatrix}$
II	$\begin{pmatrix} a & a & c \\ a & a & e \\ c & e & f \end{pmatrix}$	$\begin{pmatrix} a & b & a \\ b & d & a \\ a & a & f \end{pmatrix}$	$\begin{pmatrix} a & b & c \\ b & a & e \\ c & e & a \end{pmatrix}$	$\begin{pmatrix} a & b & b \\ b & d & a \\ b & a & f \end{pmatrix}$	$\begin{pmatrix} a & b & c \\ b & b & e \\ c & e & a \end{pmatrix}$	$\begin{pmatrix} a & b & b \\ b & d & b \\ b & b & f \end{pmatrix}$
III	$\begin{pmatrix} a & a & c \\ a & d & a \\ c & a & f \end{pmatrix}$	$\begin{pmatrix} a & b & a \\ b & d & e \\ a & e & a \end{pmatrix}$	$\begin{pmatrix} a & b & b \\ b & a & e \\ b & e & f \end{pmatrix}$	$\begin{pmatrix} a & b & c \\ b & b & a \\ c & a & f \end{pmatrix}$	$\begin{pmatrix} a & b & c \\ b & d & b \\ c & b & a \end{pmatrix}$	$\begin{pmatrix} a & b & b \\ b & d & e \\ b & e & b \end{pmatrix}$
IV	$\begin{pmatrix} a & a & c \\ a & d & e \\ c & e & a \end{pmatrix}$	$\begin{pmatrix} a & b & a \\ b & b & e \\ a & e & f \end{pmatrix}$	$\begin{pmatrix} a & b & c \\ b & a & b \\ c & b & f \end{pmatrix}$	$\begin{pmatrix} a & b & c \\ b & d & a \\ c & a & b \end{pmatrix}$	$\begin{pmatrix} a & b & c \\ b & c & e \\ c & e & a \end{pmatrix}$	$\begin{pmatrix} a & b & b \\ b & d & d \\ b & d & f \end{pmatrix}$
V	$\begin{pmatrix} a & a & c \\ a & c & e \\ c & e & f \end{pmatrix}$	$\begin{pmatrix} a & b & a \\ b & d & b \\ a & b & f \end{pmatrix}$	$\begin{pmatrix} a & b & c \\ b & a & e \\ c & e & b \end{pmatrix}$	$\begin{pmatrix} a & b & c \\ b & c & a \\ c & a & f \end{pmatrix}$	$\begin{pmatrix} a & b & c \\ b & d & c \\ c & c & a \end{pmatrix}$	$\begin{pmatrix} a & b & b \\ b & d & e \\ b & e & d \end{pmatrix}$
VI	$\begin{pmatrix} a & a & c \\ a & d & c \\ c & c & f \end{pmatrix}$	$\begin{pmatrix} a & b & a \\ b & d & e \\ a & e & b \end{pmatrix}$	$\begin{pmatrix} a & b & c \\ b & a & c \\ c & c & f \end{pmatrix}$	$\begin{pmatrix} a & b & c \\ b & d & a \\ c & a & c \end{pmatrix}$	$\begin{pmatrix} a & b & c \\ b & d & d \\ c & d & a \end{pmatrix}$	$\begin{pmatrix} a & b & b \\ b & d & e \\ b & e & e \end{pmatrix}$
VII	$\begin{pmatrix} a & a & c \\ a & d & e \\ c & e & c \end{pmatrix}$	$\begin{pmatrix} a & b & a \\ b & d & d \\ a & d & f \end{pmatrix}$	$\begin{pmatrix} a & b & c \\ b & a & e \\ c & e & c \end{pmatrix}$	$\begin{pmatrix} a & b & c \\ b & d & a \\ c & a & d \end{pmatrix}$	$\begin{pmatrix} a & b & c \\ b & d & b \\ c & b & b \end{pmatrix}$	$\begin{pmatrix} a & b & c \\ b & b & b \\ b & b & f \end{pmatrix}$
$VIII$	$\begin{pmatrix} a & a & c \\ a & d & d \\ c & d & f \end{pmatrix}$	$\begin{pmatrix} a & b & a \\ b & d & e \\ a & e & d \end{pmatrix}$	$\begin{pmatrix} a & b & c \\ b & a & e \\ a & e & e \end{pmatrix}$	$\begin{pmatrix} a & b & c \\ b & c & e \\ c & e & b \end{pmatrix}$	$\begin{pmatrix} a & b & c \\ b & c & b \\ c & b & f \end{pmatrix}$	$\begin{pmatrix} a & b & c \\ b & b & e \\ c & e & b \end{pmatrix}$
IX	$\begin{pmatrix} a & a & c \\ a & d & e \\ c & e & d \end{pmatrix}$	$\begin{pmatrix} a & b & a \\ b & d & e \\ a & e & e \end{pmatrix}$	$\begin{pmatrix} a & b & c \\ b & c & c \\ c & c & f \end{pmatrix}$	$\begin{pmatrix} a & b & c \\ b & d & c \\ c & c & b \end{pmatrix}$	$\begin{pmatrix} a & b & c \\ b & d & b \\ c & b & c \end{pmatrix}$	$\begin{pmatrix} a & b & c \\ b & b & c \\ c & c & f \end{pmatrix}$
X	$\begin{pmatrix} a & a & c \\ a & d & e \\ c & e & e \end{pmatrix}$	$\begin{pmatrix} a & b & c \\ b & d & c \\ c & c & c \end{pmatrix}$	$\begin{pmatrix} a & b & c \\ c & c & e \\ c & e & c \end{pmatrix}$	$\begin{pmatrix} a & b & c \\ b & d & d \\ c & d & b \end{pmatrix}$	$\begin{pmatrix} a & b & c \\ b & d & b \\ c & b & d \end{pmatrix}$	$\begin{pmatrix} a & b & c \\ b & b & e \\ c & e & c \end{pmatrix}$
XI	-	$\begin{pmatrix} a & b & c \\ b & d & c \\ c & c & d \end{pmatrix}$	$\begin{pmatrix} a & b & c \\ b & c & e \\ c & e & e \end{pmatrix}$	$\begin{pmatrix} a & b & c \\ b & d & d \\ c & d & d \end{pmatrix}$	$\begin{pmatrix} a & b & c \\ b & d & d \\ c & d & c \end{pmatrix}$	$\begin{pmatrix} a & b & c \\ b & b & e \\ c & e & e \end{pmatrix}$

$$U = \begin{pmatrix} c_{12}c_{13} & s_{12}c_{13} & s_{13}e^{-i\delta} \\ -s_{12}c_{23} - c_{12}s_{23}s_{13}e^{i\delta} & c_{12}c_{23} - s_{12}s_{23}s_{13}e^{i\delta} & s_{23}c_{13} \\ s_{12}s_{23} - c_{12}c_{23}s_{13}e^{i\delta} & -c_{12}s_{23} - s_{12}c_{23}s_{13}e^{i\delta} & c_{23}c_{13} \end{pmatrix}, \tag{4}$$

with $s_{ij} = \sin\theta_{ij}$ and $c_{ij} = \cos\theta_{ij}$ and

$$P_\nu = \begin{pmatrix} 1 & 0 & 0 \\ 0 & e^{i\alpha} & 0 \\ 0 & 0 & e^{i(\beta+\delta)} \end{pmatrix}, \qquad P_l = \begin{pmatrix} e^{i\varphi_e} & 0 & 0 \\ 0 & e^{i\varphi_\mu} & 0 \\ 0 & 0 & e^{i\varphi_\tau} \end{pmatrix}.$$

P_ν is the diagonal phase matrix with the two Majorana-type CP-violating phases α, β and one Dirac-type CP-violating phase δ. The phase matrix P_l is unphysical and depends on the phase convention. The matrix V is called the neutrino mixing matrix or the Pontecorvo-Maki-Nakagawa-Sakata (PMNS) matrix [14]. Using Eqs. (2) and (3), the neutrino mass matrix can be written as

$$M_\nu = P_l U P_\nu M_\nu^{\text{diag}} P_\nu^T U^T P_l^T. \tag{5}$$

The CP violation in neutrino oscillation experiments can be described through a rephasing invariant quantity, J_{CP} [15] with $J_{CP} = Im(U_{e1}U_{\mu 2}U_{e2}^* U_{\mu 1}^*)$. In the above parametrization, J_{CP} is given by

$$J_{CP} = s_{12}s_{23}s_{13}c_{12}c_{23}c_{13}^2 \sin\delta. \tag{6}$$

A. Two equalities between the elements of M_ν

The simultaneous existence of two equalities between the elements of the neutrino mass matrix implies

$$e^{i(\varphi_a+\varphi_b)}M_{\nu(ab)} - e^{i(\varphi_c+\varphi_d)}M_{\nu(cd)} = 0, \tag{7}$$

$$e^{i(\varphi_{a'}+\varphi_{b'})}M_{\nu(a'b')} - e^{i(\varphi_{c'}+\varphi_{d'})}M_{\nu(c'd')} = 0 \tag{8}$$

or

$$QM_{\nu(ab)} - M_{\nu(cd)} = 0, \tag{9}$$

$$Q'M_{\nu(a'b')} - M_{\nu(c'd')} = 0, \tag{10}$$

where

$$Q = e^{i(\varphi_a+\varphi_b-(\varphi_c+\varphi_d))}, \tag{11}$$

$$Q' = e^{i(\varphi_{a'}+\varphi_{b'}-(\varphi_{c'}+\varphi_{d'}))}. \tag{12}$$

These two conditions yield two complex equations, viz.,

$$\sum_{i=1}^{3}(QV_{ai}V_{bi} - V_{ci}V_{di})m_i = 0, \tag{13}$$

$$\sum_{i=1}^{3}(Q'V_{a'i}V_{b'i} - V_{c'i}V_{d'i})m_i = 0. \tag{14}$$

The above equations can be rewritten as

$$m_1A_1 + m_2A_2e^{2i\alpha} + m_3A_3e^{2i(\beta+\delta)} = 0, \tag{15}$$

$$m_1B_1 + m_2B_2e^{2i\alpha} + m_3B_3e^{2i(\beta+\delta)} = 0, \tag{16}$$

where

$$\begin{aligned} A_i &= (QU_{ai}U_{bi} - U_{ci}U_{di}), \\ B_i &= (Q'U_{a'i}U_{b'i} - U_{c'i}U_{d'i}), \end{aligned} \tag{17}$$

with $(i = 1, 2, 3)$. These two complex Eqs. (15) and (16) involve nine physical parameters which include m_1, m_2, m_3, θ_{12}, θ_{23}, θ_{13} and three CP-violating phases α, β and δ. In addition, there are three unphysical phases $(\varphi_e, \varphi_\mu, \varphi_\tau)$ which enter in the mass ratios as two phase differences and, in some cases, as a single phase difference. The masses m_2 and m_3 can be calculated from the mass-squared differences Δm^2_{21} and $|\Delta m^2_{23}|$ using the relations

$$m_2 = \sqrt{m_1^2 + \Delta m^2_{21}}, \qquad m_3 = \sqrt{m_2^2 + |\Delta m^2_{23}|}, \tag{18}$$

where $m_2 > m_3$ for an inverted spectrum (IS) and $m_2 < m_3$ for a normal spectrum (NS). Using the experimental inputs of the two mass-squared differences and the three mixing angles, we can constrain the other parameters. Simultaneously solving Eqs. (15) and (16) for two mass ratios, we obtain

$$\frac{m_1}{m_2}e^{-2i\alpha} = \frac{A_2B_3 - A_3B_2}{A_3B_1 - A_1B_3} \tag{19}$$

and

$$\frac{m_1}{m_3}e^{-2i\beta} = \frac{A_3B_2 - A_2B_3}{A_2B_1 - A_1B_2}e^{2i\delta}. \tag{20}$$

The magnitudes of the two mass ratios in Eqs. (19) and (20) are given by

$$\rho = \left|\frac{m_1}{m_3}e^{-2i\beta}\right|, \tag{21}$$

$$\sigma = \left|\frac{m_1}{m_2}e^{-2i\alpha}\right|, \tag{22}$$

while the CP-violating Majorana phases α and β are given by

$$\alpha = -\frac{1}{2}\arg\left(\frac{A_2B_3 - A_3B_2}{A_3B_1 - A_1B_3}\right), \tag{23}$$

$$\beta = -\frac{1}{2}\arg\left(\frac{A_3B_2 - A_2B_3}{A_2B_1 - A_1B_2}e^{2i\delta}\right). \tag{24}$$

Since Δm^2_{21} and $|\Delta m^2_{23}|$ are known experimentally, the values of mass ratios (ρ, σ) from Eqs. (21) and (22) can be used to calculate m_1. This can be done by inverting Eqs. (21) and (22) to obtain the two values of m_1, viz.,

$$m_1 = \sigma\sqrt{\frac{\Delta m^2_{21}}{1-\sigma^2}}, \qquad m_1 = \rho\sqrt{\frac{\Delta m^2_{21} + |\Delta m^2_{23}|}{1-\rho^2}}. \tag{25}$$

Similar to the case of zero textures [8], there exists a permutation symmetry between different patterns of two equalities in M_ν corresponding to the permutation in the 2–3 rows and 2–3 columns of M_ν. The corresponding permutation matrix is given by

$$P_{23} = \begin{pmatrix} 1 & 0 & 0 \\ 0 & 0 & 1 \\ 0 & 1 & 0 \end{pmatrix}. \tag{26}$$

For example, the neutrino mass matrix for class IF can be obtained from class $IIIF$ by the transformation

$$M_\nu^{IF} = P_{23}M_\nu^{IIIF}P_{23}^T. \tag{27}$$

This leads to the following relations between the parameters for the classes related by the permutation symmetry:

$$\begin{aligned} \theta_{12}^{IF} &= \theta_{12}^{IIIF}, \qquad \theta_{13}^{IF} = \theta_{13}^{IF}, \\ \theta_{23}^{IF} &= \frac{\pi}{2} - \theta_{23}^{IIIF}, \qquad \delta^{IF} = \delta^{IIIF} - \pi. \end{aligned} \tag{28}$$

The textures related by the 2–3 permutation symmetry are

$$IB \leftrightarrow IVA,\ IC \leftrightarrow ID,\ IE \leftrightarrow IIIC,\ IF \leftrightarrow IIIF,\ IIA \leftrightarrow IIIB,\ IIB \leftrightarrow IIIA,\ IIE \leftrightarrow VIIC,\ IIID \leftrightarrow VID,\ IIIE \leftrightarrow VIC,$$
$$IVB \leftrightarrow VIIA,\ IVC \leftrightarrow VE,\ IVD \leftrightarrow VD,\ IVE \leftrightarrow VC,\ IVF \leftrightarrow VIF,\ VA \leftrightarrow VIB,\ VB \leftrightarrow VIA,\ VIE \leftrightarrow VIIIC,\ VIIB \leftrightarrow XA,$$
$$VIIE \leftrightarrow IXC,\ VIIF \leftrightarrow XB,\ VIIIA \leftrightarrow IXB,\ VIIIB \leftrightarrow IXA,\ VIIIE \leftrightarrow IXD,\ VIIIF \leftrightarrow XC,\ IXE \leftrightarrow IXF,\ XD \leftrightarrow XIC,$$
$$XE \leftrightarrow XIB,\ XIE \leftrightarrow XIF. \tag{29}$$

The remaining textures

$$IA,\quad IIC,\quad IID,\quad IIF,\quad VF,\quad VIID,\quad VIIID,\quad XF,\quad XID \tag{30}$$

transform unto themselves. It is interesting to note that class VF is the widely studied μ-τ symmetric texture structure [16].

B. Two equalities between the cofactors of M_ν

The simultaneous existence of two equalities between the cofactors of the neutrino mass matrix implies

$$\begin{aligned}&(-1^{(\gamma\xi)})(e^{i(\varphi_a+\varphi_b+\varphi_c+\varphi_d)}M_{\nu(ab)}M_{\nu(cd)}\\&\quad- e^{i(\varphi_f+\varphi_g+\varphi_m+\varphi_n)}M_{\nu(fg)}M_{\nu(mn)})\\&\quad-(-1^{(\zeta\eta)})(e^{i(\varphi_p+\varphi_q+\varphi_r+\varphi_s)}M_{\nu(pq)}M_{\nu(rs)}\\&\quad- e^{i(\varphi_t+\varphi_u+\varphi_v+\varphi_w)}M_{\nu(tu)}M_{\nu(vw)})=0,\end{aligned} \tag{31}$$

$$\begin{aligned}&(-1^{(\gamma'\xi')})(e^{i(\varphi_{a'}+\varphi_{b'}+\varphi_{c'}+\varphi_{d'})}M_{\nu(a'b')}M_{\nu(c'd')}\\&\quad- e^{i(\varphi_{f'}+\varphi_{g'}+\varphi_{m'}+\varphi_{n'})}M_{\nu(f'g')}M_{\nu(m'n')})\\&\quad-(-1^{(\zeta'\eta')})(e^{i(\varphi_{p'}+\varphi_{q'}+\varphi_{r'}+\varphi_{s'})}M_{\nu(p'q')}M_{\nu(r's')}\\&\quad- e^{i(\varphi_{t'}+\varphi_{u'}+\varphi_{v'}+\varphi_{w'})}M_{\nu(t'u')}M_{\nu(v'w')})=0,\end{aligned} \tag{32}$$

or

$$\begin{aligned}&(-1^{(\gamma\xi)})(Q_1M_{\nu(ab)}M_{\nu(cd)}-Q_2M_{\nu(fg)}M_{\nu(mn)})\\&\quad-(-1^{(\zeta\eta)})(Q_3M_{\nu(pq)}M_{\nu(rs)}-Q_4M_{\nu(tu)}M_{\nu(vw)})=0,\end{aligned} \tag{33}$$

$$\begin{aligned}&(-1^{(\gamma'\xi')})(Q'_1M_{\nu(a'b')}M_{\nu(c'd')}-Q'_2M_{\nu(f'g')}M_{\nu(m'n')})\\&\quad-(-1^{(\zeta'\eta')})(Q'_3M_{\nu(p'q')}M_{\nu(r's')}-Q'_4M_{\nu(t'u')}M_{\nu(v'w')})=0.\end{aligned} \tag{34}$$

It is inherent in the properties of cofactors that when we substitute φ_j $(j = e, \mu, \tau)$, $Q_1 = Q_2$, $Q_3 = Q_4$, $Q'_1 = Q'_2$, and $Q'_3 = Q'_4$. Thus, we have

$$\begin{aligned}&(-1^{(\gamma\xi)})Q_1(M_{\nu(ab)}M_{\nu(cd)}-M_{\nu(fg)}M_{\nu(mn)})\\&\quad-(-1^{(\zeta\eta)})Q_3(M_{\nu(pq)}M_{\nu(rs)}-M_{\nu(tu)}M_{\nu(vw)})=0,\end{aligned} \tag{35}$$

$$\begin{aligned}&(-1^{(\gamma'\xi')})Q'_1(M_{\nu(a'b')}M_{\nu(c'd')}-M_{\nu(f'g')}M_{\nu(m'n')})\\&\quad-(-1^{(\zeta'\eta')})Q'_3(M_{\nu(p'q')}M_{\nu(r's')}-M_{\nu(t'u')}M_{\nu(v'w')})=0,\end{aligned} \tag{36}$$

or

$$\begin{aligned}&(-1^{(\gamma\xi)})Q(M_{\nu(ab)}M_{\nu(cd)}-M_{\nu(fg)}M_{\nu(mn)})\\&\quad-(-1^{(\zeta\eta)})(M_{\nu(pq)}M_{\nu(rs)}-M_{\nu(tu)}M_{\nu(vw)})=0,\end{aligned} \tag{37}$$

$$\begin{aligned}&(-1^{(\gamma'\xi')})Q'(M_{\nu(a'b')}M_{\nu(c'd')}-M_{\nu(f'g')}M_{\nu(m'n')})\\&\quad-(-1^{(\zeta'\eta')})(M_{\nu(p'q')}M_{\nu(r's')}-M_{\nu(t'u')}M_{\nu(v'w')})=0,\end{aligned} \tag{38}$$

where $Q = \frac{Q_1}{Q_3}$ and $Q' = \frac{Q'_1}{Q'_3}$.

The above two conditions take the following form when expressed in terms of mixing matrix elements and mass eigenvalues:

$$\begin{aligned}&\sum_{l,k=1}^{3}\{(-1^{(\gamma\xi)})Q(V_{al}V_{bl}V_{ck}V_{dk}-V_{fl}V_{gl}V_{mk}V_{nk})\\&\quad-(-1^{(\zeta\eta)})(V_{pl}V_{ql}V_{rk}V_{sk}-V_{tl}V_{ul}V_{vk}V_{wk})\}m_lm_k=0,\end{aligned} \tag{39}$$

$$\begin{aligned}&\sum_{l,k=1}^{3}\{(-1^{(\gamma'\xi')})Q'(V_{a'l}V_{b'l}V_{c'k}V_{d'k}-V_{f'l}V_{g'l}V_{m'k}V_{n'k})\\&\quad-(-1^{(\zeta'\eta')})(V_{p'l}V_{q'l}V_{r'k}V_{s'k}-V_{t'l}V_{u'l}V_{v'k}V_{w'k})\}\\&\quad\times m_lm_k=0.\end{aligned} \tag{40}$$

The above equations can be rewritten as

$$m_1m_2C_3e^{2i\alpha}+m_2m_3C_1e^{2i(\alpha+\beta+\delta)}+m_3m_1C_2e^{2i(\beta+\delta)}=0, \tag{41}$$

$$m_1m_2D_3e^{2i\alpha}+m_2m_3D_1e^{2i(\alpha+\beta+\delta)}+m_3m_1D_2e^{2i(\beta+\delta)}=0, \tag{42}$$

where

$$\begin{aligned}C_h=&(-1^{(\gamma\xi)})Q(U_{al}U_{bl}U_{ck}U_{dk}-U_{fl}U_{gl}U_{mk}U_{nk})\\&-(-1^{(\zeta\eta)})(U_{pl}U_{ql}U_{rk}U_{sk}-U_{tl}U_{ul}U_{vk}U_{wk})\\&+(l\leftrightarrow k),\end{aligned} \tag{43}$$

$$D_h = (-1^{(\gamma' \xi')}) Q' (U_{a'l} U_{b'l} U_{c'k} U_{d'k} - U_{f'l} U_{g'l} U_{m'k} U_{n'k}) - (-1^{(\zeta' \eta')}) (U_{p'l} U_{q'l} U_{r'k} U_{s'k} - U_{t'l} U_{u'l} U_{v'k} U_{w'k}) + (l \leftrightarrow k), \quad (44)$$

with (h, l, k) as the cyclic permutation of (1,2,3). Simultaneously solving Eqs. (41) and (42) for the two mass ratios, we obtain

$$\frac{m_1}{m_2} e^{-2i\alpha} = \frac{C_3 D_1 - C_1 D_3}{C_2 D_3 - C_3 D_2} \quad (45)$$

and

$$\frac{m_1}{m_3} e^{-2i\beta} = \frac{C_2 D_1 - C_1 D_2}{C_3 D_2 - C_2 D_3} e^{2i\delta}. \quad (46)$$

The magnitudes of the above two mass ratios are given by

$$\rho = \left| \frac{m_1}{m_3} e^{-2i\beta} \right|, \quad (47)$$

$$\sigma = \left| \frac{m_1}{m_2} e^{-2i\alpha} \right|, \quad (48)$$

while the CP-violating Majorana phases α and β are given by

$$\alpha = -\frac{1}{2} \arg \left(\frac{C_3 D_1 - C_1 D_3}{C_2 D_3 - C_3 D_2} \right), \quad (49)$$

$$\beta = -\frac{1}{2} \arg \left(\frac{C_2 D_1 - C_1 D_2}{C_3 D_2 - C_2 D_3} e^{2i\delta} \right). \quad (50)$$

Again there exists a permutation symmetry between the different classes of two equalities of cofactors in M_ν which corresponds to the permutation in the 2–3 rows and 2–3 columns of M_ν. The classification of these texture structures is similar to the case of two equalities between elements of M_ν.

III. NUMERICAL RESULTS

The current experimental constraints on neutrino parameters at 1, 2 and 3σ [17] are given in Table II. The two values of m_1 obtained from Eqs. (21) and (22) for TEE [or Eqs. (48) and (49) for TEC] must be equal to within the errors of the oscillation parameters, for the simultaneous existence of two equalities between elements or cofactors of M_ν, respectively. The known oscillation parameters are varied randomly within their 3σ experimental ranges. The unconstrained Dirac-type CP-violating phase δ is varied randomly within its full possible range. For the numerical analysis we generate 10^7 points (10^8 when the number of allowed points is small). For most of the viable cases we obtain a lower bound on the effective Majorana mass of the electron neutrino (M_{ee}). The observation of neutrinoless double beta (NDB) decay would signal lepton number violation and imply the Majorana nature of neutrinos; for recent reviews on NDB decay, see Ref. [18]. M_{ee}, which determines the rate of NDB decay, is given by

TABLE II. Current neutrino oscillation parameters from global fits [17]. The upper (lower) row corresponds to a normal (inverted) spectrum, with $\Delta m^2_{31} > 0$ ($\Delta m^2_{31} < 0$).

Parameter	Mean$^{(+1\sigma,+2\sigma,+3\sigma)}_{(-1\sigma,-2\sigma,-3\sigma)}$
$\Delta m^2_{21}[10^{-5}\ \text{eV}^2]$	$7.62^{(+0.19,+0.39,+0.58)}_{(-0.19,-0.35,-0.5)}$
$\Delta m^2_{31}[10^{-3}\ \text{eV}^2]$	$2.55^{(+0.06,+0.13,+0.19)}_{(-0.09,-0.19,-0.24)}$, $(-2.43^{(+0.09,+0.19,+0.24)}_{(-0.07,-0.15,-0.21)})$
$\sin^2\theta_{12}$	$0.32^{(+0.016,+0.03,+0.05)}_{(-0.017,-0.03,-0.05)}$
$\sin^2\theta_{23}$	$0.613^{(+0.022,+0.047,+0.067)}_{(-0.04,-0.233,-0.25)}$, $(0.60^{(+0.026,+0.05,+0.07)}_{(-0.031,-0.210,-0.230)})$
$\sin^2\theta_{13}$	$0.0246^{(+0.0028,+0.0056,+0.0076)}_{(-0.0029,-0.0054,-0.0084)}$, $(0.0250^{(+0.0026,+0.005,+0.008)}_{(-0.0027,-0.005,-0.008)})$

$$M_{ee} = |m_1 c_{12}^2 c_{13}^2 + m_2 s_{12}^2 c_{13}^2 e^{2i\alpha} + m_3 s_{13}^2 e^{2i\beta}|. \quad (51)$$

NDB decay provides a window to probe the neutrino mass scale. Part of the Heidelberg-Moscow Collaboration claimed a positive signal for NDB decay corresponding to $M_{ee} = (0.11\text{–}0.56)$ eV at 95% C.L. [19]. However, this claim was subsequently criticized in Ref. [20]. The results reported in Ref. [19] will be checked in the currently running and forthcoming NDB decay experiments. There are a large number of projects, such as CUORICINO [21], CUORE [22], GERDA [23], MAJORANA [24], SuperNEMO [25], EXO [26], and GENIUS [27], which aim to achieve a sensitivity up to 0.01 eV for M_{ee}. In our numerical analysis, we take the upper limit of M_{ee} to be 0.5 eV. Cosmological observations put an upper bound on the sum of neutrino masses

$$\Sigma = \sum_{i=1}^{3} m_i. \quad (52)$$

The nine-year WMAP data alone restrict Σ to be less than 1.3 eV (95% C.L.) [28]. The combined WMAP + eCMB + BAO + H_0 data limit $\Sigma < 0.44$ eV at 95% C.L. [28]. However, these limits strongly depend on the details of the model considered and the data set used. In our numerical analysis we have taken the upper limit of Σ to be 0.9 eV.

A. Numerical results for TEE

In this section, we present the numerical results for textures with two equalities between the elements of the neutrino mass matrix. The main outcomes of our analysis are

TABLE III. The numerical predictions for the phenomenologically viable textures in the case of two equalities between the elements of M_ν.

Texture	Spectrum	M_{ee} (eV)	Lower bound on mass scale (eV)	Majorana phases
IA	NS	0.004–0.12	0.001	$\alpha = 0°$–$70°$, $110°$–$180°$
	IS	0.02–0.16	0.001	$\alpha = 50°$–$70°$, $110°$–$130°$
IB (IVA)	NS	0.006–0.14	0.007	⋯
	IS	0.02–0.18	0.007	$\alpha = 40°$–$140°$
IC (ID)	NS	0.02–0.12	0.023	⋯
	IS	0.01–0.14	0.007	$\alpha = 50°$–$130°$
IE (IIIC)	NS	0.004–0.30	0.0030	⋯
	IS	0.01–0.30	0.0004	⋯
IF (IIIF)	NS	0.004–0.30	0.007	⋯
	IS	0.02–0.30	0.001	⋯
IIA (IIIB)	NS	0.007–0.12	0.006	$\alpha = 30°$–$80°$, $100°$–$150°$
	IS	0.02–0.16	0.040	$\alpha = 60°$–$120°$
IIB (IIIA)	NS	0.01–0.11	0.017	$\alpha = 20°$–$160°$
	IS	0.02–0.16	0.020	$\alpha = 40°$–$130°$
IIC	NS	0.01–0.30	0.0100	⋯
	IS	0.01–0.22	0.0033	$\alpha = 20°$–$180°$
IID	NS	0.01–0.30	0.01	$\alpha = 0°$–$80°$, $100°$–$180°$
	IS	0.01–0.30	0.01	⋯
IIE (VIIC)	NS	0.015–0.20	0.02	⋯
	IS	0.01–0.18	0.02	$\alpha = 20°$–$160°$
IIF	NS	0.01–0.30	0.025	⋯
	IS	0.03–0.30	0.004	⋯
IIID (VID)	NS	0.01–0.30	0.025	⋯
	IS	0.01–0.30	0.025	⋯
IVB (VIIA)	NS	0.001–0.16	0.0040	$\alpha = 0°$–$160°$
	IS	0.02–0.16	0.0005	$\alpha = 50°$–$75°$, $105°$–$130°$
IVC (VE)	NS	0.005–0.25	0.025	⋯
	IS	0.02–0.30	0.030	⋯
IVE (VC)	NS	0.01–0.18	0.016	⋯
	IS	0.02–0.14	0.016	$\alpha = 40°$–$140°$
IVF (VIF)	NS	0.003–0.30	0.0033	$\alpha = 0°$–$20°$, $160°$–$180°$
	IS	0.01–0.30	0.00475	⋯
VA (VIB)	NS	0.001–0.16	0.005	⋯
	IS	0.02–0.14	0.005	$\alpha = 40°$–$140°$
VB (VIA)	NS	0.0012–0.09	0.0165	$\alpha = 40°$–$140°$
VIE (VIIIC)	NS	0.006–0.18	0.005	⋯
	IS	0.010–0.18	0.0002	$\alpha = 30°$–$140°$
VIIB (XA)	NS	0–0.12	0.0001	⋯
	IS	0.02–0.12	0.0002	$\alpha = 40°$–$140°$
VIID	NS	0.01–0.30	0.0100	⋯
	IS	0.01–0.30	0.006	⋯
VIIE (IXC)	NS	0.005–0.16	0.0300	$\alpha = 50°$–$130°$
	IS	0.03–0.12	0.0003	$\alpha = 20°$–$80°$, $100°$–$160°$
VIIF (XB)	NS	0.002–0.14	0.0140	$\alpha = 40°$–$160°$
	IS	0.02–0.14	0.0001	$\alpha = 20°$–$160°$
VIIIA (IXB)	NS	0.0004–0.10	0	⋯
	IS	0.02–0.14	0.0001	$\alpha = 40°$–$140°$
VIIIB (IXA)	NS	0.001–0.16	0.0001	⋯
	IS	0.02–0.16	0.0010	$\alpha = 50°$–$80°$, $100°$–$130°$
VIIID	NS	0.005–0.30	0.025	⋯
	IS	0.028–0.30	0.001	⋯

TABLE III. (*Continued*)

Texture	Spectrum	M_{ee} (eV)	Lower bound on mass scale (eV)	Majorana phases
VIIIE (IXD)	NS	0.005–0.14	0.0270	$\alpha = 50°$–$130°$
	IS	0.03–0.12	0.0002	$\alpha = 20°$–$80°$, $100°$–$160°$
VIIIF (XC)	NS	0.005–0.30	0.0200	...
	IS	0.02–0.30	0.0003	...
IXE (IXF)	IS	0.03–0.05	0.005	$\alpha = 30°$–$50°$, $130°$–$150°$
XD (XIC)	NS	0.002–0.18	0.0010	...
	IS	0.02–0.13	0.0005	$\alpha = 0°$–$70°$, $110°$–$180°$
XE (XIB)	NS	0.002–0.30	0.017	...
	IS	0.02–0.30	0.001	...
XF	NS	0.005–0.30	0.025	...
	IS	0.025–0.30	0.002	$\alpha = 0°$–$80°$, $100°$–$180°$
XID	IS	0.01–0.055	0.0005	$\beta = 70°$–$110°$
XIE (XIF)	NS	0.001–0.12	0.0080	...
	IS	0.01–0.18	0.0002	...

(i) Five textures, viz., *IIIE*, *VIC*, *IVD*, *VD*, and *VF*, are excluded by the experimental data.

(ii) Textures *IXE*, *IXF*, and *XID* lead to an inverted spectrum only.

(iii) Textures *VB* and *VIA* satisfy a normal spectrum only.

(iv) The allowed points for the following textures are very few: *IA*, *IE*, *IIIC*, *IIA*, *IIIB*, *IID* for an inverted spectrum; *IIC*, *XE*, *XIB*, *VIIE*, *IXC* for

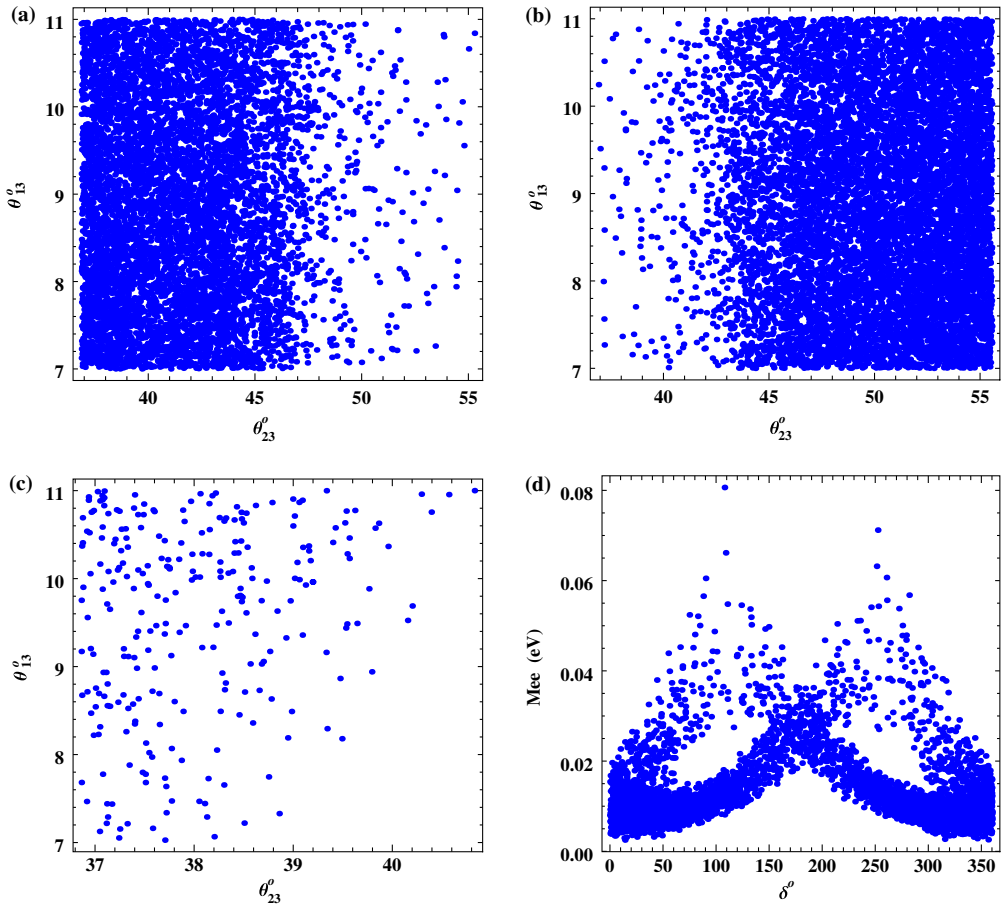

FIG. 1 (color online). The TEE correlation plots for classes *IF*(*a*)(NS), *IIIF*(*b*)(NS), *IIIB*(*c*)(IS), and *VB*(*d*)(NS).

a normal spectrum; and $VIIF$, XC for both inverted and normal spectrums. We have generated 10^8 points for these textures.

(v) All the viable textures except IA(NS), IXE, IXF, and XID allow a quasidegenerate spectrum.

(vi) The value of M_{ee} is bounded from below for most of the viable textures.

(vii) It is found that the smallest neutrino mass cannot be zero for any of the allowed textures except for $VIIIA$(NS) and IXB(NS).

(viii) For textures IE, $IIIC$, IF, $IIIF$, IIF, IVF, and VIF, a nonvanishing reactor mixing angle is an inherent property, since for $\theta_{13} = 0$ these textures predict $m_1 = m_2$, which contradicts the experimental observations.

The numerical results for all the presently viable classes are summarized in Table III. We have presented some of the interesting results in Figs. 1–3. Figures 1(a) and 1(b) show the 2–3 interchange symmetry between classes IF and $IIIF$. From Fig. 1(c), we can see that for IS in class $IIIB$, θ_{23} remains below maximal. Figure 1(d) shows the correlation plot between δ and M_{ee} for class VB(NS). Figures 2(a) and 2(b) show the plots for class IVF(NS), which is one of the most predictive classes in this analysis. The predictions for δ strongly depend on the value of M_{ee}. Class $VIIID$ predicts θ_{23} to be near maximal, as shown in Figs. 2(c) and 2(d). For class IXE(IS), there is a strong correlation between the Dirac-type phase δ and the Majorana-type phase β. Moreover, M_{ee} is restricted to a very small range in this case [Figs. 3(a) and 3(b)]. For class XF(NS), θ_{23} near its maximal value is more probable [Fig. 3(c)]. As shown in Fig. 3(d), there is a strong correlation between the two Majorana-type CP-violating phases for class XID(IS).

B. Numerical results for TEC

The numerical results for two equalities between the cofactors of the neutrino mass matrix are presented here. The main outcomes are

(i) Five textures, viz., $IIIE$, VIC, IVD, VD, and VF, are excluded by the experimental data.

(ii) Textures IXE, IXF, and XID lead to a normal spectrum only.

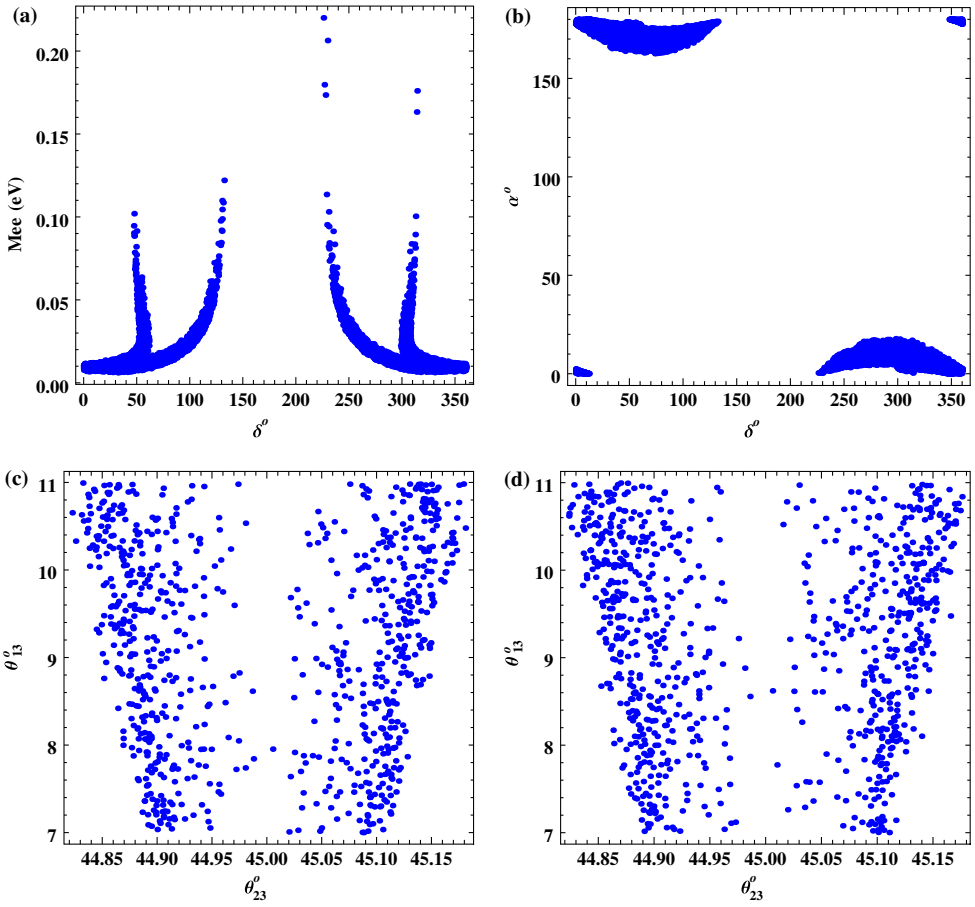

FIG. 2 (color online). The TEE correlation plots for classes $IVF(a)$(NS), $IVF(b)$(NS), $VIIID(c)$(NS), and $VIIID(d)$(IS).

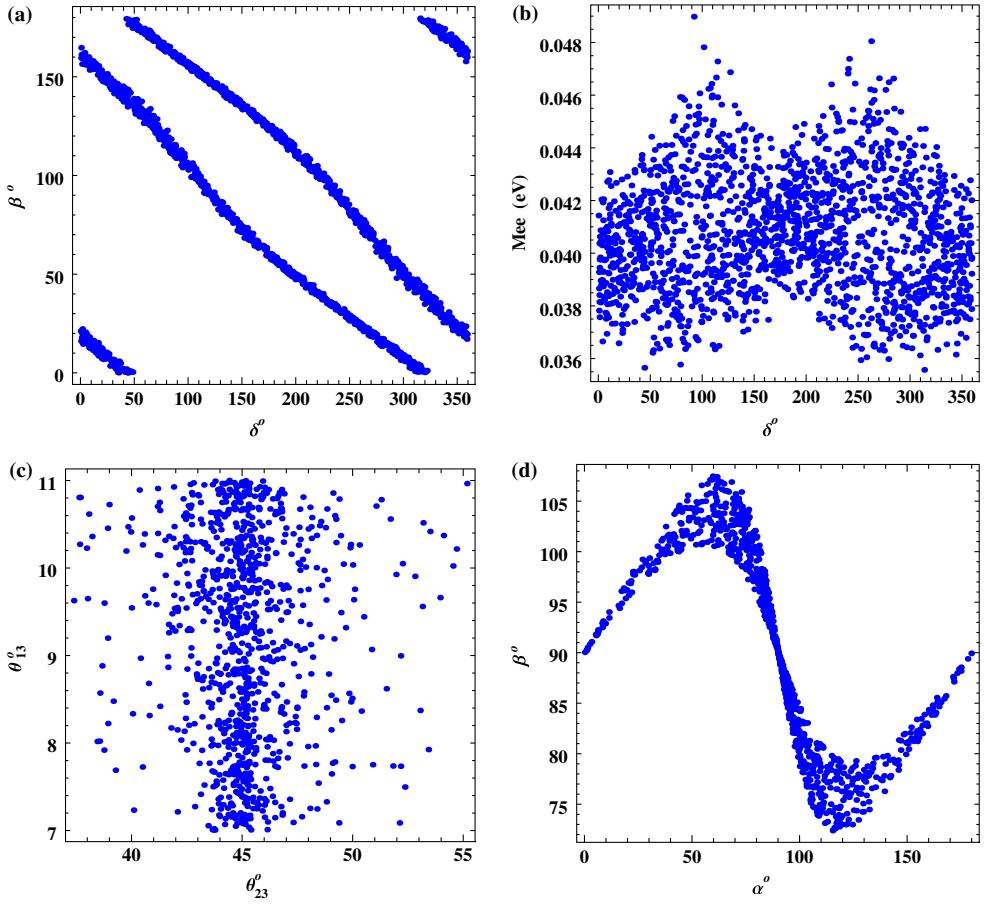

FIG. 3 (color online). The TEE correlation plots for classes $IXE(a)$(IS), $IXE(b)$(IS), $XF(c)$(NS), and $XID(d)$(IS).

(iii) Textures VB and VIA hold for an inverted spectrum only.

(iv) The allowed points for the following textures are very few: IC, ID, IIC, $IIID$, VID, $VIID$, $VIIE$, IXC, $VIIF$, XB, $VIIIB$, IXA, $VIIIE$, IXD, $VIIIF$, XC, XD, XIC, XE, XIB, XIE, XIF for an inverted spectrum; IIA, $IIIB$ for a normal spectrum; and IVC, VE for both inverted and normal spectrums. We have generated 10^8 points for these textures.

(v) All the viable textures except IXE, IXF, and XID allow a quasidegenerate spectrum.

(vi) For most of the viable textures, we obtain a lower bound on M_{ee}, but for texture XID this parameter can only have a vanishing value.

(vii) It is found that the smallest neutrino mass cannot be zero for any of the allowed textures.

(viii) For textures IE, $IIIC$, IF, $IIIF$, IIF, IVF, and VIF, a nonvanishing reactor mixing angle is an inherent property.

The numerical results for all the classes which satisfy the present experimental data are summarized in Table IV. Some of the interesting results are plotted in Figs. 4–6. Figures 4(a) and 4(b) show correlation plots for classes $IIIB$ and IIA(NS) which are related by 2–3 interchange symmetry, as the value of θ_{23} is below maximal for class $IIIB$, whereas for class IIA it is above maximal. Figures 4(c) and 4(d) correspond to class $VIIID$ for NS and IS, respectively, and the atmospheric mixing angle θ_{23} is restricted to the proximity of its maximal value for IS. In Fig. 5, we have depicted the correlation plots for class IVF, which is one of the most predictive classes of TEC; Figs. 5(a)–5(c) correspond to IS, while Fig. 5(d) corresponds to NS. The Dirac-type phase δ is correlated with M_{ee} [Fig. 5(a)]. It is clear from Fig. 5(b) that this class is necessarily CP-violating because the Jarlskog CP-violation rephasing invariant cannot vanish in this case. Figures 6(a) and 6(b) correspond to class IXE(NS) for which the unknown parameter M_{ee} is restricted to a very small range. In Fig. 6(c), we have plotted m_1 and m_3 for class $VIID$(NS) for which the quasidegenerate limit is allowed, as is the case for most of the classes included in this analysis. The two Majorana-type CP-violating phases α and β for class XID are plotted in Fig. 6(d). For this class, only a normal spectrum is allowed and the unknown parameter M_{ee} can only have a vanishing value because the M_R corresponding to this texture has a vanishing cofactor corresponding to the (e, e) entry, which manifests as a vanishing M_{ee} in the neutrino mass matrix M_ν. Comparing the numerical results of TEE and TEC, we

TABLE IV. The numerical predictions for the phenomenologically viable textures in the case of two equalities between the cofactors of M_ν.

Texture	Spectrum	M_{ee} (eV)	Lower bound on mass scale (eV)	Majorana phases
IA	NS	0.0004–0.07	0.003	$\alpha = 50°$–$130°$
	IS	0.02–0.08	0.001	$\alpha = 0°$–$70°$, $110°$–$180°$
IB (IVA)	NS	0.005–0.16	0.015	$\alpha = 40°$–$140°$
	IS	0.015–0.14	0.010	⋯
IC (ID)	NS	0.001–0.14	0.018	$\alpha = 50°$–$130°$
	IS	0.035–0.18	0.020	⋯
IE (IIIC)	NS	0.001–0.30	0.010	⋯
	IS	0.02–0.30	0.006	⋯
IF (IIIF)	NS	0.003–0.30	0.001	⋯
	IS	0.010–0.30	0.010	⋯
IIA (IIIB)	NS	0.02–0.16	0.040	$\alpha = 60°$–$120°$
	IS	0.02–0.16	0.006	$\alpha = 40°$–$80°$, $100°$–$140°$
IIB (IIIA)	NS	0.01–0.12	0.025	$\alpha = 50°$–$140°$
	IS	0.02–0.14	0.018	$\alpha = 20°$–$160°$
IIC	NS	0.003–0.30	0.010	$\alpha = 20°$–$160°$
	IS	0.025–0.25	0.010	⋯
IID	NS	0.001–0.30	0.015	⋯
	IS	0.030–0.30	0.010	⋯
IIE (VIIC)	NS	0.004–0.12	0.020	$\alpha = 20°$–$160°$
	IS	0.020–0.14	0.020	⋯
IIF	NS	0.003–0.30	0.001	⋯
	IS	0.010–0.30	0.030	⋯
IIID (VID)	NS	0.005–0.25	0.025	⋯
	IS	0.025–0.30	0.025	⋯
IVB (VIIA)	NS	0.001–0.16	0.003	$\alpha = 50°$–$80°$, $100°$–$130°$
	IS	0.010–0.16	0.008	$\alpha = 40°$–$140°$
IVC (VE)	NS	0.01–0.30	0.028	⋯
	IS	0.01–0.30	0.028	⋯
IVE (VC)	NS	0.007–0.16	0.018	$\alpha = 40°$–$140°$
	IS	0.01–0.18	0.020	⋯
IVF (VIF)	NS	0–0.20	0.0001	⋯
	IS	0.04–0.22	0.0001	$\alpha = 0°$–$20°$, $160°$–$180°$
VA (VIB)	NS	0.002–0.14	0.004	$\alpha = 40°$–$140°$
	IS	0.02–0.16	0.010	$\alpha = 30°$–$150°$
VB (VIA)	IS	0.01–0.08	0.020	$\alpha = 40°$–$140°$
VIE (VIIIC)	NS	0.0001–0.16	0.010	$\alpha = 40°$–$140°$
	IS	0.01–0.14	0.010	⋯
VIIB (XA)	NS	0–0.14	0.002	$\alpha = 40°$–$140°$
	IS	0.01–0.16	0.001	⋯
VIID	NS	0.002–0.30	0.015	⋯
	IS	0.025–0.30	0.010	⋯
VIIE (IXC)	NS	0.001–0.16	0.001	$\alpha = 0°$–$80°$, $100°$–$180°$
	IS	0.01–0.18	0.030	$\alpha = 50°$–$130°$
VIIF (XB)	NS	0.001–0.14	0.003	⋯
	IS	0.010–0.18	0.014	$\alpha = 20°$–$160°$
VIIIA (IXB)	NS	0–0.08	0.001	$\alpha = 40°$–$140°$
	IS	0.01–0.16	0.001	⋯
VIIIB (IXA)	NS	0–0.12	0.001	$\alpha = 50°$–$130°$
	IS	0.01–0.18	0.002	⋯
VIIID	NS	0.002–0.30	0.002	⋯
VIIID	IS	0.015–0.30	0.027	⋯

TABLE IV. (*Continued*)

Texture	Spectrum	M_{ee} (eV)	Lower bound on mass scale (eV)	Majorana phases
VIIIE (IXD)	NS	0.001–0.14	0.001	...
	IS	0.01–0.20	0.025	$\alpha = 50°$–$130°$
VIIIF (XC)	NS	0.002–0.30	0.0014	...
	IS	0.01–0.30	0.0200	...
IXE (IXF)	NS	0.005–0.03	0.004	$\alpha = 20°$–$50°$, $130°$–$160°$
XD (XIC)	NS	0.001–0.10	0.0010	$\alpha \neq 90°$
	IS	0.01–0.18	0.0135	...
XE (XIB)	NS	0.001–0.30	0.001	...
	IS	0.01–0.30	0.020	...
XF	NS	0.002–0.30	0.001	$\alpha = 0°$–$80°$, $100°$–$180°$
	IS	0.01–0.30	0.025	...
XID	NS	0	0.0005	$\alpha = 60°$–$120°$
XIE (XIF)	NS	0.001–0.16	0.001	...
	IS	0.01–0.16	0.010	$\alpha = 20°$–$160°$

find that the phenomenological predictions for a texture are in general similar for both cases (i.e., TEE and TEC) except for the mass hierarchy which gets reversed. For example, the disallowed classes are the same in both cases. The textures which only satisfy NS in the case of TEE get replaced by IS for TEC and vice versa. The textures for which a nonvanishing reactor mixing angle is an inherent property are the same in both cases. Thus, the distinguishing feature between TEE and TEC for a texture, in general, is the neutrino mass hierarchy. The reason for the

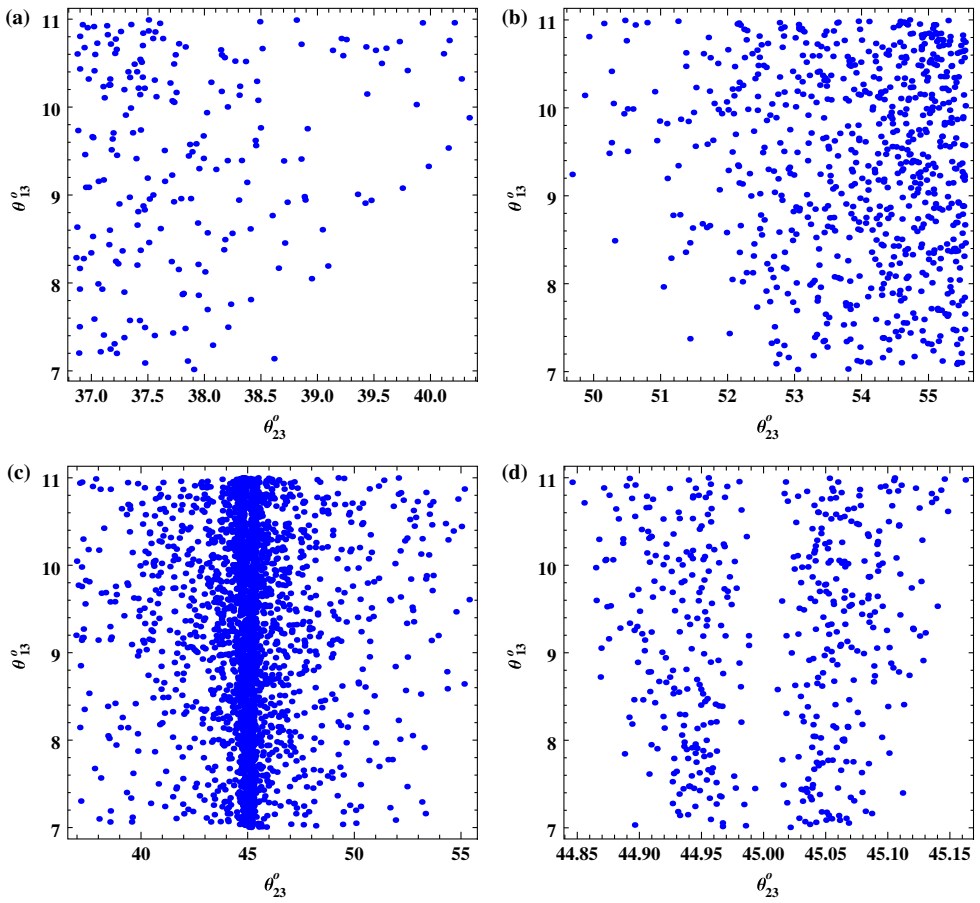

FIG. 4 (color online). The TEC correlation plots for classes *IIIB*(*a*)(NS), *IIA*(*b*)(NS), *VIIID*(*c*)(NS), and *VIIID*(*d*)(IS).

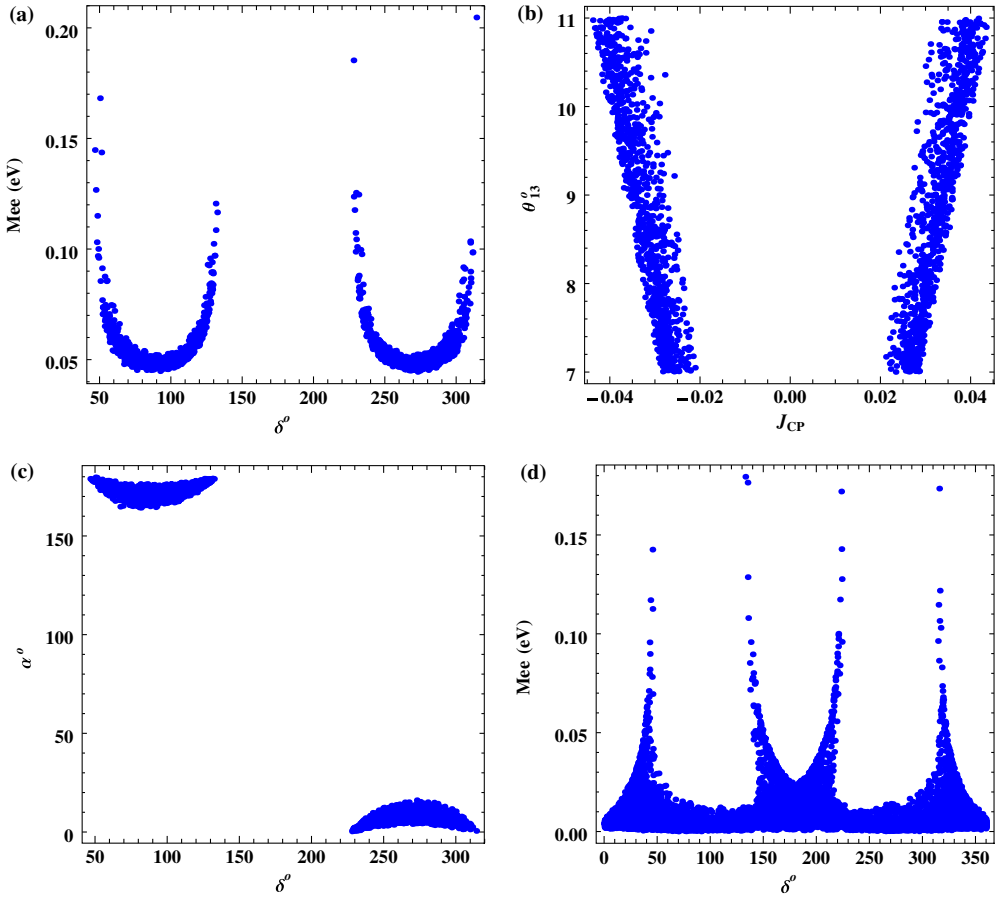

FIG. 5 (color online). The TEC correlation plots for classes $IVF(a, b, c)$(IS) and $IVF(d)$(NS).

similar phenomenological predictions (and for the reversal of the mass hierarchy) of corresponding textures of TEE and TEC can be understood in the following way. The diagonalization equation of M_ν [Eq. (2)] is

$$M_\nu = V' M_\nu^{\text{diag}} V'^T. \tag{53}$$

Taking the inverse of M_ν gives

$$M_\nu^{-1} = V'^* (M_\nu^{\text{diag}})^{-1} V'^\dagger. \tag{54}$$

For two equalities between the elements of M_ν, M_ν^{-1} has two equalities between the cofactors and vice versa. Thus, TEE and TEC textures are just the inverse of each other. It can be seen from the above equations that the mixing matrices are complex conjugates of each other. Thus, they span the same parameter space for mixing angles and it is expected that the corresponding textures of TEC and TEE have similar phenomenological predictions for the mixing angles. However, it is not necessary that the allowed values of mixing angles are exactly the same in both cases because the mass eigenvalues are inversely related and different regions of mixing angles may be allowed from the whole parameter space when we use the input of mass squared differences.

IV. SYMMETRY REALIZATION

Here we present a simple $A_4 \times Z_2$ model for one of the cases, viz., IIC of TEC studied in this analysis. All the leptonic fields are assigned to the triplet representation of A_4. The transformations of various fields are given in Table V. These transformation properties lead to the following $A_4 \times Z_2$ invariant Lagrangian for the leptons:

$$\begin{aligned}\mathcal{L} = {} & Y_1(\bar{D}_{e_L} e_R + \bar{D}_{\mu_L} \mu_R + \bar{D}_{\tau_L} \tau_R)_{\underline{1}} \phi_1 + Y_2(\bar{D}_{e_L} e_R + \omega \bar{D}_{\mu_L} \mu_R + \omega^2 \bar{D}_{\tau_L} \tau_R)_{\underline{1}'} \phi_3 + Y_3(\bar{D}_{e_L} e_R + \omega^2 \bar{D}_{\mu_L} \mu_R \\ & + \omega \bar{D}_{\tau_L} \tau_R)_{\underline{1}''} \phi_2 + Y_4(\bar{D}_{e_L} \nu_{e_R} + \bar{D}_{\mu_L} \nu_{\mu_R} + \bar{D}_{\tau_L} \nu_{\tau_R})_{\underline{1}} \tilde{\phi}_4 + \frac{M_M}{2}(\nu_{e_R}^T C^{-1} \nu_{e_R} + \nu_{\mu_R}^T C^{-1} \nu_{\mu_R} + \nu_{\tau_R}^T C^{-1} \nu_{\tau_R})_{\underline{1}} \\ & + \frac{Y_{M_1}}{2}[(\nu_{\mu_R}^T C^{-1} \nu_{\tau_R} + \nu_{\tau_R}^T C^{-1} \nu_{\mu_R}) \chi_1 + (\nu_{\tau_R}^T C^{-1} \nu_{e_R} + \nu_{e_R}^T C^{-1} \nu_{\tau_R}) \chi_2 + (\nu_{e_R}^T C^{-1} \nu_{\mu_R} + \nu_{\mu_R}^T C^{-1} \nu_{e_R}) \chi_3]_{\underline{1}} + \text{H.c.},\end{aligned} \tag{55}$$

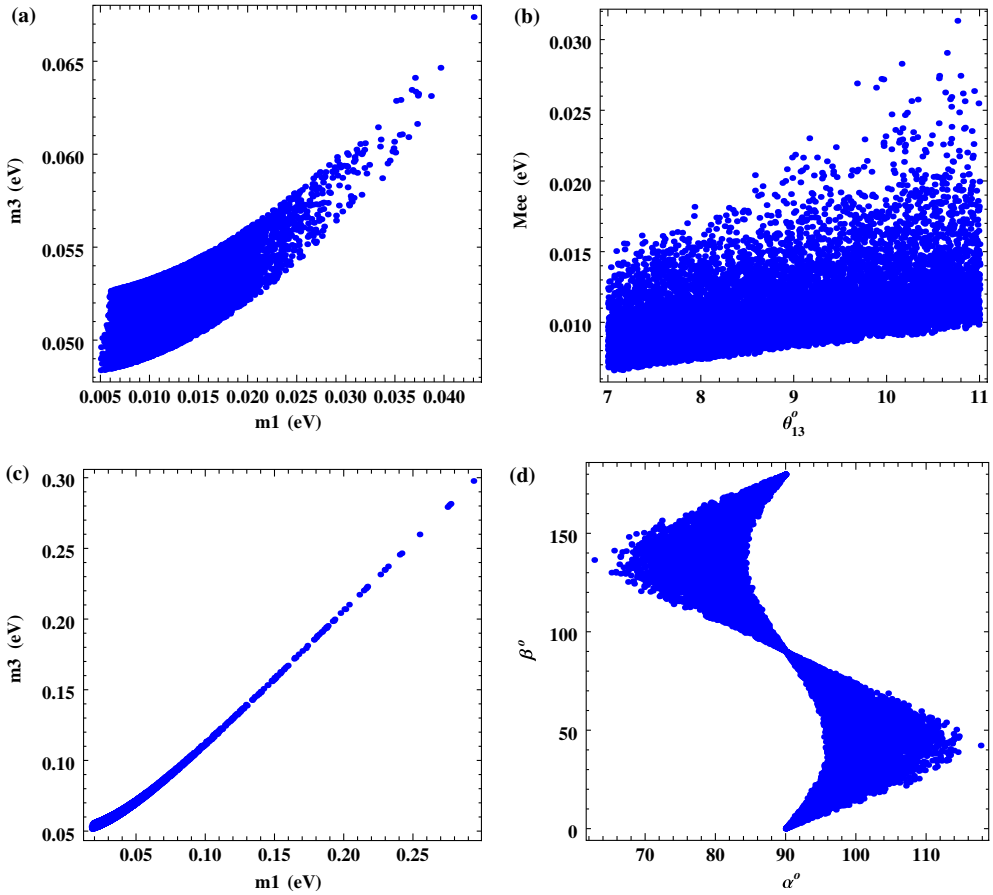

FIG. 6 (color online). The TEC correlation plots for classes $IXE(a)$(NS), $IXE(b)$(NS), $VIID(c)$(NS), and $XID(d)$(NS).

where $\tilde{\phi}_4 = i\tau_2\phi_4^*$. The Z_2 symmetry is used to prevent the coupling of the Higgs doublet ϕ_4 with the charged leptons so that it only contributes to the Dirac neutrino mass matrix and vice versa. When the various Higgs fields acquire nonzero vacuum expectation values (VEVs), the $A_4 \times Z_2$ invariant Yukawa Lagrangian leads to a diagonal charged lepton mass matrix

$$M_l = \begin{pmatrix} m_e & 0 & 0 \\ 0 & m_\mu & 0 \\ 0 & 0 & m_\tau \end{pmatrix}, \tag{56}$$

where $m_e = Y_1\langle\phi_1\rangle_o + Y_2\langle\phi_3\rangle_o + Y_3\langle\phi_2\rangle_o$, $m_\mu = Y_1\langle\phi_1\rangle_o + \omega Y_2\langle\phi_3\rangle_o + \omega^2 Y_3\langle\phi_2\rangle_o$, and $m_\tau = Y_1\langle\phi_1\rangle_o + \omega^2 Y_2\langle\phi_3\rangle_o + \omega Y_3\langle\phi_2\rangle_o$. The Dirac neutrino mass matrix is proportional to the 3×3 identity matrix

$$M_D = Y_4\langle\Phi_4\rangle_o \mathbf{I}. \tag{57}$$

The right-handed Majorana mass matrix M_R has the form

$$M_R = \begin{pmatrix} a & b & c \\ b & a & d \\ c & d & a \end{pmatrix}. \tag{58}$$

The diagonal entries in M_R come from the bare Majorana mass term and the off-diagonal entries arise via the Yukawa couplings with χ_i. Since the off-diagonal elements of M_R are supposed to be all different, the scalar potential must be rich enough for the VEVs of χ_i to be all different. After the type-I seesaw, the effective neutrino mass matrix M_ν has TEC corresponding to the 11, 22, and 33 entries.

For class IIC of TEE, the transformations of various fields are given in Table VI. We have pointed out earlier that such textures in M_ν may arise through a type-II

TABLE V. Transformation properties of various fields for case IIC of TEC.

Fields	D_{l_L}	l_R	ν_{l_R}	ϕ_1	ϕ_2	ϕ_3	ϕ_4	χ_i
$SU(2)_L$	2	1	1	2	2	2	2	1
A_4	**3**	**3**	**3**	**1**	**1′**	**1″**	**1**	**3**
Z_2	+	+	−	+	+	+	−	+

TABLE VI. Transformation properties of various fields for case IIC of TEE.

Fields	D_{l_L}	l_R	ν_{l_R}	ϕ_1	ϕ_2	ϕ_3	$\triangle_i$	$\triangle_4$
$SU(2)_L$	2	1	1	2	2	2	3	3
A_4	**3**	**3**	**3**	**1**	**1′**	**1″**	**3**	**1**

seesaw, for which we need to add four Higgs $SU(2)_L$ triplets $\triangle_i$, and no right-handed neutrino fields are needed. Three of the $SU(2)_L$ triplets transform in combination as the A_4 triplet and the fourth one is a singlet of A_4. A diagonal charged lepton mass matrix arises exactly in the same way as in the case IIC of TEC, since the transformation properties of charged lepton fields remain the same as in the earlier case. The A_4 invariant Lagrangian for neutrinos is

$$\begin{aligned}\mathcal{L} = \frac{M_{L_1}}{2}[&(D^T_{\mu_L} C^{-1} i\tau_2 \triangle_1 D_{\tau_L} + D^T_{\tau_L} C^{-1} i\tau_2 \triangle_1 D_{\mu_L}) \\ &+ (D^T_{\tau_L} C^{-1} i\tau_2 \triangle_2 D_{e_L} + D^T_{e_L} C^{-1} i\tau_2 \triangle_2 D_{\tau_L}) \\ &+ (D^T_{e_L} C^{-1} i\tau_2 \triangle_3 D_{\mu_L} + D^T_{\mu_L} C^{-1} i\tau_2 \triangle_3 D_{e_L})]_{\underline{\mathbf{1}}} \\ &+ \frac{M_{L_2}}{2}(D^T_{e_L} C^{-1} i\tau_2 \triangle_4 D_{e_L} + D^T_{\mu_L} C^{-1} i\tau_2 \triangle_4 D_{\mu_L} \\ &+ D^T_{\tau_L} C^{-1} i\tau_2 \triangle_4 D_{\tau_L})_{\underline{\mathbf{1}}} + \text{H.c.}, \end{aligned} \tag{59}$$

where the $SU(2)_L$ triplets are written in 2×2 matrix notation:

$$\triangle = \begin{pmatrix} H^+ & \sqrt{2}H^{++} \\ \sqrt{2}H^0 & -H^+ \end{pmatrix}. \tag{60}$$

When the neutral components of the $SU(2)_L$ triplet Higgs fields acquire small but nonzero and distinct VEVs, we get the neutrino mass matrix having the form IIC of TEE

$$M_\nu = \begin{pmatrix} a & b & c \\ b & a & d \\ c & d & a \end{pmatrix}. \tag{61}$$

V. SUMMARY

We studied in detail the implications of the presence of two equalities between the elements or the cofactors of the neutrino mass matrix. Two equalities between the elements of the neutrino mass matrix can be obtained through the type-II seesaw mechanism, whereas two equalities between the cofactors are obtained through the type-I seesaw mechanism when the right-handed neutrino mass matrix has two equalities between elements and the Dirac neutrino mass matrix is proportional to the unit matrix. A total of 65 texture structures are possible for each case. Predictions for M_{ee} are given for the allowed texture structures. This parameter is expected to be measured in the forthcoming NDB decay experiments. To illustrate how such texture structures can be realized, we presented a simple A_4 model for the texture structure IIC. The viability of these textures suggests that there are still rich, unexplored structures of the neutrino mass matrix from both the phenomenological and theoretical points of view. Future data from various experiments, along with the input of flavor symmetry, will help in deciding the form of the neutrino mass matrix.

ACKNOWLEDGMENTS

The research work of S. D. and L. S. is supported by the University Grants Commission, Government of India *vide* Grant No. 34-32/2008 (SR). R. R. G. acknowledges the financial support provided by the Council for Scientific and Industrial Research (CSIR), Government of India.

APPENDIX: THE GROUP A_4

A_4 is the group of even permutations of four objects having 12 elements. Geometrically, it can be viewed as the group of rotational symmetries of the tetrahedron. A_4 has four inequivalent irreducible representations (IRs) which are three singlets $\mathbf{1}$, $\mathbf{1}'$, and $\mathbf{1}''$, and one triplet $\mathbf{3}$. A_4 is generated by two generators S and T such that

$$S^2 = T^3 = (ST)^3 = 1. \tag{A1}$$

The one-dimensional unitary IRs are

$$\begin{aligned}&\mathbf{1} \quad S = 1 \quad T = 1, \qquad \mathbf{1}' \quad S = 1 \quad T = \omega, \\ &\qquad\qquad \mathbf{1}'' \quad S = 1 \quad T = \omega^2. \end{aligned} \tag{A2}$$

The three-dimensional unitary IR is

$$S = \begin{pmatrix} 1 & 0 & 0 \\ 0 & -1 & 0 \\ 0 & 0 & -1 \end{pmatrix}, \qquad T = \begin{pmatrix} 0 & 1 & 0 \\ 0 & 0 & 1 \\ 1 & 0 & 0 \end{pmatrix}. \tag{A3}$$

The multiplication rules of the IRs are as follows:

$$\mathbf{1}' \otimes \mathbf{1}' = \mathbf{1}'', \qquad \mathbf{1}'' \otimes \mathbf{1}'' = \mathbf{1}', \qquad \mathbf{1}' \otimes \mathbf{1}'' = \mathbf{1}. \tag{A4}$$

The product of two $\mathbf{3}$'s gives

$$\mathbf{3} \otimes \mathbf{3} = \mathbf{1} \oplus \mathbf{1}' \oplus \mathbf{1}'' \oplus \mathbf{3}_s \oplus \mathbf{3}_a, \tag{A5}$$

where s (a) denotes a symmetric (antisymmetric) product. Let (x_1, x_2, x_3) and (y_1, y_2, y_3) denote the basis vectors of two $\mathbf{3}$'s. Then the IRs obtained from their products are

$$(\mathbf{3} \otimes \mathbf{3})_{\mathbf{1}} = x_1y_1 + x_2y_2 + x_3y_3, \tag{A6}$$

$$(\mathbf{3} \otimes \mathbf{3})_{\mathbf{1}'} = x_1y_1 + \omega x_2y_2 + \omega^2 x_3y_3, \tag{A7}$$

$$(\mathbf{3} \otimes \mathbf{3})_{\mathbf{1}''} = x_1y_1 + \omega^2 x_2y_2 + \omega x_3y_3, \tag{A8}$$

$$(\mathbf{3} \otimes \mathbf{3})_{\mathbf{3}_s} = (x_2y_3 + x_3y_2, x_3y_1 + x_1y_3, x_1y_2 + x_2y_1), \tag{A9}$$

$$(\mathbf{3} \otimes \mathbf{3})_{\mathbf{3}_a} = (x_2y_3 - x_3y_2, x_3y_1 - x_1y_3, x_1y_2 - x_2y_1). \tag{A10}$$

[1] K. Abe *et al.* (T2K Collaboration), Phys. Rev. Lett. **107**, 041801 (2011).

[2] P. Adamson *et al.* (MINOS Collaboration), Phys. Rev. Lett. **107**, 181802 (2011).

[3] Y. Abe *et al.* (Double Chooz Collaboration), Phys. Rev. Lett. **108**, 131801 (2012).

[4] F. P. An *et al.* (Daya Bay Collaboration), Phys. Rev. Lett. **108**, 171803 (2012).

[5] Soo-Bong Kim (RENO Collaboration), Phys. Rev. Lett. **108**, 191802 (2012).

[6] P. F. Harrison, D. H. Perkins, and W. G. Scott, Phys. Lett. B **530**, 167 (2002); P. F. Harrison and W. G. Scott, Phys. Lett. B **535**, 163 (2002); Z.-z. Xing, Phys. Lett. B **533**, 85 (2002).

[7] P. H. Frampton, S. L. Glashow, and D. Marfatia, Phys. Lett. B **536**, 79 (2002); Z.-z. Xing, Phys. Lett. B **530**, 159 (2002); B. R. Desai, D. P. Roy, and A. R. Vaucher, Mod. Phys. Lett. A **18**, 1355 (2003); S. Dev, S. Kumar, S. Verma, and S. Gupta, Nucl. Phys. **B784**, 103 (2007); S. Dev, S. Kumar, S. Verma, and S. Gupta, Phys. Rev. D **76**, 013002 (2007); M. Randhawa, G. Ahuja, and M. Gupta, Phys. Lett. B **643**, 175 (2006); G. Ahuja, S. Kumar, M. Randhawa, M. Gupta, and S. Dev, Phys. Rev. D **76**, 013006 (2007); S. Kumar, Phys. Rev. D **84**, 077301 (2011); P. O. Ludl, S. Morisi, and E. Peinado, Nucl. Phys. **B857**, 411 (2012); D. Meloni and G. Blankenburg, Nucl. Phys. **B867**, 749 (2013); W. Grimus and P. O. Ludl, arXiv:1208.4515.

[8] H. Fritzsch, Z.-z. Xing, and S. Zhou, J. High Energy Phys. 09 (2011) 083.

[9] L. Lavoura, Phys. Lett. B **609**, 317 (2005); E. I. Lashin and N. Chamoun, Phys. Rev. D **78**, 073002 (2008); **80**, 093004 (2009); S. Dev, S. Verma, S. Gupta, and R. R. Gautam, Phys. Rev. D **81**, 053010 (2010); S. Dev, S. Gupta, and R. R. Gautam, Mod. Phys. Lett. A **26**, 501 (2011); S. Dev, S. Gupta, R. R. Gautam, and L. Singh, Phys. Lett. B **706**, 168 (2011); T. Araki, J. Heeck, and J. Kubo, J. High Energy Phys. 07 (2012) 083.

[10] S. Kaneko, H. Sawanaka, and M. Tanimoto, J. High Energy Phys. 08 (2005) 073; S. Goswami, S. Khan, and A. Watanabe, Phys. Lett. B **693**, 249 (2010); S. Dev, S. Verma, and S. Gupta, Phys. Lett. B **687**, 53 (2010); S. Dev, S. Gupta, and R. R. Gautam, Phys. Rev. D **82**, 073015 (2010).

[11] W. Konetschny and W. Kummer, Phys. Lett. **70B**, 433 (1977); T. P. Cheng and L. F. Li, Phys. Rev. D **22**, 2860 (1980); J. Schechter and J. W. F. Valle, Phys. Rev. D **22**, 2227 (1980); G. Lazarides, Q. Shafi, and C. Wetterich, Nucl. Phys. **B181**, 287 (1981); R. N. Mohapatra and G. Senjanovic, Phys. Rev. D **23**, 165 (1981).

[12] P. Minkowski, Phys. Lett. **67B**, 421 (1977); T. Yanagida, *Proceedings of the Workshop on the Unified Theory and the Baryon Number in the Universe*, edited by O. Sawada and A. Sugamoto (KEK, Tsukuba, 1979), p. 95; M. Gell-Mann, P. Ramond, and R. Slansky, *Complex Spinors and Unified Theories in Supergravity*, edited by P. Van Nieuwenhuizen and D. Z. Freedman (North Holland, Amsterdam, 1979), p. 315; R. N. Mohapatra and G. Senjanovic, Phys. Rev. Lett. **44**, 912 (1980).

[13] G. L. Fogli, E. Lisi, A. Marrone, and A. Palazzo, Prog. Part. Nucl. Phys. **57**, 742 (2006).

[14] B. Pontecorvo, Zh. Eksp. Teor. Fiz. **33**, 549 (1957) [Sov. Phys. JETP **6**, 429 (1957)]; **34**, 247 (1958); **53**, 1717 (1967); Z. Maki, M. Nakagawa, and S. Sakata, Prog. Theor. Phys. **28**, 870 (1962).

[15] C. Jarlskog, Phys. Rev. Lett. **55**, 1039 (1985).

[16] For a recent review, see W. Grimus and L. Lavoura, arXiv:1207.1678.

[17] M. Tortola, J. W. F. Valle, and D. Vanegas, Phys. Rev. D **86**, 073012 (2012).

[18] F. T. Avignone III, S. R. Elliott, and J. Engel, Rev. Mod. Phys. **80**, 481 (2008); W. Rodejohann, Int. J. Mod. Phys. E **20**, 1833 (2011); J. J. Gomez-Cadenas, J. Martin-Albo, M. Mezzetto, F. Monrabal, and M. Sorel, Riv. Nuovo Cimento **35**, 29 (2012); S. M. Bilenky and C. Giunti, Mod. Phys. Lett. A **27**, 1230015 (2012).

[19] H. V. Klapdor-Kleingrothaus, A. Dietz, H. L. Harney, and I. V. Krivosheina, Mod. Phys. Lett. A **16**, 2409 (2001).

[20] F. Feruglio, A. Strumia, and F. Vissani, Nucl. Phys. **B637**, 345 (2002); C. E. Aalseth *et al.*, Mod. Phys. Lett. A **17**, 1475 (2002).

[21] C. Arnaboldi *et al.* (CUORICINO Collaboration), Phys. Lett. B **584**, 260 (2004).

[22] C. Arnaboldi *et al.*, Nucl. Instrum. Methods Phys. Res., Sect. A **518**, 775 (2004).

[23] I. Abt *et al.* (GERDA Collaboration), arXiv:hep-ex/0404039.

[24] R. Gaitskell *et al.* (Majorana Collaboration), arXiv:nucl-ex/0311013.

[25] A. S. Barabash (NEMO Collaboration), Czech. J. Phys. **52**, 567 (2002).

[26] M. Danilov *et al.*, Phys. Lett. B **480**, 12 (2000).

[27] H. V. Klapdor-Kleingrothaus *et al.*, Eur. Phys. J. A **12**, 147 (2001).

[28] G. Hinshaw *et al.*, arXiv:1212.5226.